Revue RAMReS – Sciences Appliquées et de l'Ingénieur
RAMReS 2025 - *Published Online 2026* - http://publication.lecames.org/
Vol. 7(1), pp. 21- 27, Online January 2026

Vol. 7
ISSN 2630-1164
December 2025

CRUFAOCI

Full Length Research Paper

Three-dimensional analysis of the impact of grain size and recombination rate at grain boundaries on the extension of the space charge zone (ZCE) of a polycrystalline silicon monofacial photocell under multispectral illumination.

Mayoro Dieye[1*], Mamadou Mbaye [2], Dame Diao [3], Awa Dieye [4], Nacire Mbengue [5]
[1,3]Solar Energy Materials and Système Laboratory (LASES), Université Cheikh Anta Diop 2 – Dakar, SENEGAL
[2,4,5]Semiconductor Optoelectronics Group (GOES) , Université Cheikh Anta Diop 2 – Dakar, SENEGAL

Received June 2025 – Accepted October 2025

**Corresponding author. yoroma90@gmail.com*

Abstract:

In this article, we investigate the extension of the space charge region within a three-dimensional bifacial polysilicon photocell subjected to multispectral illumination in a static regime. Our analysis focuses on the influence of grain size and recombination rates at grain boundaries on the characteristics of this region.

By solving the continuity equation, we derive the expression for the density of excess minority charge carriers, from which we subsequently obtain the relative density of these carriers as a function of depth. This framework allows us to delineate how the relative density of minority charge carriers correlates with the extension of the space charge zone.

Our findings indicate that the extension $Z_{0,av}$ of the space charge zone can be modeled as exhibiting the properties of a plane capacitor. Specifically, we explore how variations in grain size and recombination rates at grain boundaries affect the overall extension of this zone in the polycrystalline silicon cell.

We observe that an increase in recombination velocities at grain boundaries results in a reduction of the diffusion capacity, transitioning from $Sg_b = 20$ cm/s. Conversely, enlarging the grain size from $C_{av} = 1.331\text{x}10^4$ nF/cm^{-2} to $C_{av} = 5.04\text{x}10^3$ nF/cm^{-2}. enhances the diffusion capacity, reaching a peak value of g = 20 µm to g = 3,00 x 10^2 µm enhances the diffusion capacity, reaching a peak value of $C_{av} = 3.50\ \text{x}10^5$ nF/cm^{-2}. Through a detailed analysis of the relative densities of minority charge carriers as a function of depth z within the base, we are able to articulate the extension $Z_{0,av}$ of the space charge zone. This parameter serves as a critical indicator of the photocell's performance and overall quality.

In summary, our research elucidates the interplay between microstructural parameters and the fundamental electrical properties of bifacial polysilicon photocells, providing valuable insights for future advancements in photovoltaic technology.

Keyword : Photocell -Irradiation -Rate of recombination at grain boundaries-Grain size, Polycrystalline.

Cite this article:
Mayoro Dieye, Mamadou Mbaye, Dame Diao, Awa Dieye, Nacire Mbengue (2025). Three-dimensional analysis of the impact of grain size and recombination rate at grain boundaries on the extension of the space charge zone (ZCE) of a polycrystalline silicon monofacial photocell under multispectral illumination. Revue RAMReS – Sci. Appl. & de l'Ing., Vol. 7(1), pp. 21-27. ISSN 2630-1164.

1. Introduction

Several advanced techniques have been employed to characterize silicon materials and ascertain both phenomenological and electrical parameters, aiming to enhance the efficiency of solar cells. Among these techniques, some are developed within the static regime [1], while others operate within the dynamic frequency domain [2].

Comprehensive studies on the capacity of the space charge region [3][4] have been conducted in three dimensions [1][5]-[8] across both regimes. These investigations have focused on elucidating the intricate interplay between microstructural characteristics and the resultant electrical behavior of silicon-based photovoltaic devices.

Our contribution specifically involves the determination of the relative density of minority charge carriers within a three-dimensional silicon photocell subjected to irradiation under multispectral illumination in a static regime. This approach allows us to deepen our understanding of the space charge dynamics and their impact on the photocell's performance, thereby providing critical insights into optimizing solar cell technologies for enhanced energy conversion efficiency.

2. Theoretical Analysis

In an n+-p-p+ polycrystalline solar cell [9], the presence of numerous small individual grains significantly influences its performance, particularly through grain boundary effects, which can function as electron-hole traps. These interactions at the grain boundaries are critical in determining the overall efficiency of the solar cell.

For the simulation of physical processes, we consider a fibrously oriented columnar grain structure, as depicted in the cross-section in fig.1. Fig.2 illustrates the configuration of the bifacial solar cell in a planar orientation, highlighting its structural nuances.

Focusing on an isolated grain, as shown in fig.3, we conducted detailed calculations to analyze the variation of key parameters such as irradiation intensity (K_l) and photon flux (ϕ) [4]. This analysis aims to explore how different illumination modes affect the electrical characteristics and efficiency of the solar cell. By understanding these relationships, we can gain insights into optimizing the design and operational strategies for enhancing solar cell performance.

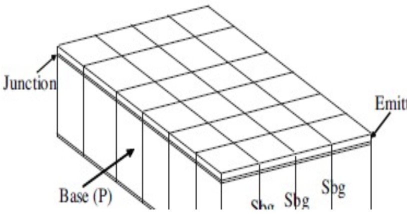

Figure.1: Fibrously oriented **Figure.2: Bifacial solar cell**

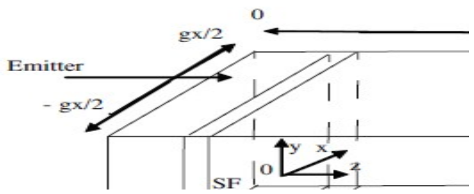

Figure.3: Schematic of an isolated grain

2.1. Excess Minority Carriers Density

Considering the emitter as a dead (non active) area, the excess minority carrier distribution in the base, seen as a greater contribution to the photo-conversion, is derived from the continuity equation [5-9] [10,11] [27,28]:

$$D(Kl,\phi)\times\left[\frac{\partial^2\delta(x,y,z)}{\partial x^2}+\frac{\partial^2\delta(x,y,z)}{\partial y^2}+\frac{\partial^2\delta(x,y,z)}{\partial z^2}\right]-\frac{\delta(x,y,z)}{\tau}+G(z)=0$$

[Eq. 1]

$D(Kl,\phi)$ is the diffusion coefficient in the presence of irradiation. It is expressed as follows:

$$D(Kl,\phi)=\frac{L(Kl,\phi)^2}{\tau} \qquad \text{[Eq. 2]}$$

In this expression, G(z) represents the generation rate of the minority charge carriers in the base [25] whose expression is given by the following equation:

$$G(z)=\sum_{i=1}^{3} a_i\times\exp(-b_i\times z) \qquad \text{[Eq. 3]}$$

The ai and bi values are the tabulated values from the modeling of the absorption spectrum of the solar cell for AM 1.5 [10] [16] [17].

L depend on the irradiation energy Φ and the damage coefficient Kl through the following expression [13]-[15]:

$$L(Kl,\phi)=\sqrt{\frac{1}{\frac{1}{L_0^2}+Kl\times\phi}} \qquad \text{[Eq. 4]}$$

L_0 is the diffusion length without irradiation.

The solution of the equation can be written as follows [5] [12] [17]:

$$\delta(x,y,z)=\sum_k\sum_j Z_{k,j}(z)\times\cos(C_k\times x).\cos(C_j\times y)$$

[Eq. 5]

k, j: are the indices relating to the x and y directions respectively.

The eigenvalues Ck and Cj are obtained from the conditions at the grain boundaries $\pm\frac{gx}{2}$ and $\pm\frac{gy}{2}$ [5] [18] [22] [23]:

$$\left[\frac{\partial\delta(x,y,z)}{\partial x}\right]_{x=\pm\frac{g_x}{2}}=\mp\frac{Sgb}{D(Kl,\phi)}\delta\left(\pm\frac{g_x}{2},y,z\right) \qquad \text{[Eq. 6]}$$

$$\left[\frac{\partial\delta(x,y,z)}{\partial y}\right]_{y=\pm\frac{g_y}{2}}=\mp\frac{Sgb}{D(Kl,\phi)}\delta\left(x\pm\frac{g_y}{2},z\right) \qquad \text{[Eq. 7]}$$

gx is the width of the grain, gy is the length of the grain, Sgb [16] is the rate of recombination at the grain boundaries [25].

From equations [Eq. 6] and [Eq. 7] we obtain two transcendent equations [20] which are:

$$\tan\left(C_k\times\frac{g_x}{2}\right)=\frac{Sgb}{2.C_k\times D(Kl,\phi)} \qquad \text{[Eq. 8]}$$

$$\tan\left(C_j\times\frac{g_y}{2}\right)=\frac{Sgb}{2.C_j\times D(Kl,\phi)} \qquad \text{[Eq. 9]}$$

Replacing δ(x, y, z) in the continuity equation and the fact that the cosine function is orthogonal, we obtain the following differential equation:

$$Z_{k,j}=A_{k,j}\times\cosh\left(\frac{z}{L_{k,j}}\right)+B_{k,j}\times\sinh\left(\frac{z}{L_{k,j}}\right)-\sum_{i=1}^{3}K_{i,j,k}\times\exp(-b_i\times z)$$

[Eq. 10]

Où $K_{i,j,k}=\frac{L_{k,j}^2}{D_{k,j}\times\left[b_i^2\times L_{k,j}^2-1\right]}\times a_i$ [Eq. 11]

Avec : $L_{k,j}=\left[C_k^2+C_j^2+\frac{1}{L(Kl,\phi)^2}\right]^{-\frac{1}{2}}$ [Eq. 12]

Et

$$D_{k,j} = D(Kl,\phi)\times\frac{[C_k \times g_x + \sin(C_k \times g_x)][C_j \times g_y + \sin(C_j \times g_y)]}{16.\sin\left(C_k \times \frac{g_x}{2}\right).\sin\left(C_j \times \frac{g_y}{2}\right)}$$

[Eq. 13]

The coefficients $A_{k,j}$ and $B_{k,j}$ are calculated from the following boundary conditions [5] [19] [20]:

- At the junction (z=0) :

$$\left[\frac{\partial\delta(x,y,z)}{\partial z}\right]_{z=0} = \frac{Sf}{D(Kl,\phi)}\delta(x,y,0) \qquad \text{[Eq. 14]}$$

Sf is the junction recombination velocity, written as [5] [8] [19] [20] [24] Sf = Sf_0 + Sf_j with Sf_0 being the intrinsic junction recombination velocity related to the shunt resistance due to losses occurring across the junction and Sf_j is the imposed junction recombination velocity due external load. It defines the current flow that is the operating point of the cell. For each illumination mode, the intrinsic junction recombination velocity was calculated using the method described in [5] [8] [19] [20] [24].

- On the back side (z=*w*b) :

$$\left[\frac{\partial\delta(x,y,z)}{\partial z}\right]_{z=0} = -\frac{Sb}{D(Kl,\phi)}\delta(x,y,\omega b) \qquad \text{[Eq. 15]}$$

Sb is the back surface recombination velocity. It quantifies the rate at which excess minority carriers are lost at the back surface of the cell [5] [8] [19] [20] [24]. The derivation of the photocurrent with respect to Sf, provides for each illumination mode the expression of Sb, as in [5] [8] [19] [20] [24].

$$A_{k,j} = \sum_{i=1}^{3} K_{i,k,j}\times\frac{\frac{1}{L_{k,j}}.\left(\frac{Sf}{D(Kl,\phi)} - b_i\right)\times\exp(-b_i\times\omega b) + Y_{k,j}\left(\frac{Sf}{D(Kl,\phi)} + b_i\right)}{\frac{Sf\times Y_{k,j}}{D(Kl,\phi)} + \frac{X_{k,j}}{L_{k,j}}}$$

[Eq. 16]

$$B_{k,j} = \sum_{i=1}^{3} K_{i,k,j}\times\frac{\frac{Sf}{D(Kl,\phi)}.\left(\frac{Sb}{D(Kl,\phi)} - b_i\right)\times\exp(-b_i\times\omega b) + X_{k,j}\left(\frac{Sf}{D(Kl,\phi)} + b_i\right)}{\frac{Sf\times Y_{k,j}}{D(Kl,\phi)} + \frac{X_{k,j}}{L_{k,j}}}$$

[Eq. 17]

With : $X_{k,j} = \frac{1}{L_{k,j}}\times\sinh\left(\frac{\omega b}{L_{k,j}}\right) + \frac{Sb}{D(Kl,\phi)}\times\cosh\left(\frac{\omega b}{L_{k,j}}\right)$

[Eq. 18]

$$Y_{k,j} = \frac{1}{L_{k,j}}\times\cosh\left(\frac{\omega b}{L_{k,j}}\right) + \frac{Sb}{D(Kl,\phi)}\times\sinh\left(\frac{\omega b}{L_{k,j}}\right)$$

[Eq. 19]

2.1 Relative density of minority charge carriers

The relative density of excess minority charge carriers in the base is defined as follows:

$$\delta_{rel}(z,Sf,Sb,g,Sgb,Kl,\phi) = \frac{\delta(z,Sf,Sb,g,Sgb,Kl,\phi)}{\delta_{max}}$$

[Eq. 20]

2.2. Diffusion capability of the photocell at the junction-base interface

When the solar cell is illuminated, we witness a storage of opposing charges on either side of the transmitter-base junction. This leads to the establishment of a capacitor whose scattering capacity varies according to the effects of illumination on the solar cell [4] [8] [23].

The expression of the latter is defined by [18] :

$$C(Sf,Sb,g,Sgb,Kl,\phi) = \frac{q}{V_T}\times\left[\delta(Sf,Sb,g,Sgb,Kl,\phi) + \frac{n_i^2}{N_b}\right]$$

[Eq. 21]

$V_T = \frac{k\times T}{q}$ is the thermal tension, k is the Boltzmann constant, Nb is the doping rate of the base and neither the intrinsic concentration of the carriers.

3. Résultats

3.1. Determination of Space Load Area Extension $Z_{0,av}$

We propose a model for a bifacial photocell, conceptualizing the solar cell as a flat capacitor with a variable thickness $Z_{0,av}(Sf,g,Sgb,Kl,\phi)$, allowing it to expand or contract based on operational conditions.

Our objective is to determine the extension of the space charge region when one parameter is varied while the others remain constant.

To have $Z_{0,av}(Sf,g,Sgb,Kl,\phi)$ this bifacial photocell operates under polychromatic illumination and is characterized by several critical parameters: the recombination rate at the junction, grain size, recombination rate at the grain boundaries, irradiation energy, and the damage coefficient. To analyze the effects of these parameters, we plot the relative density of minority charge carriers, establishing $Z_{0,av}(Sf,g,Sgb,Kl,\phi)$ a reference for our study.

Following this calculation. This relationship is vital for understanding how variations in the physical properties of the photocell influence its electrical performance. $Z_{0,av}(Sf,g,Sgb,Kl,\phi)$ is made.

Fig.4 illustrates the relative density of minority charge carriers within the bifacial photocell when illuminated from the front surface. This curve provides a crucial reference that highlights how carrier density varies with depth in the base layer, offering insights into the charge distribution dynamics and the overall efficiency of the solar cell.

In summary, this comprehensive analysis enhances our understanding of the factors affecting bifacial photocell performance, laying the groundwork for future innovations in photovoltaic technology.

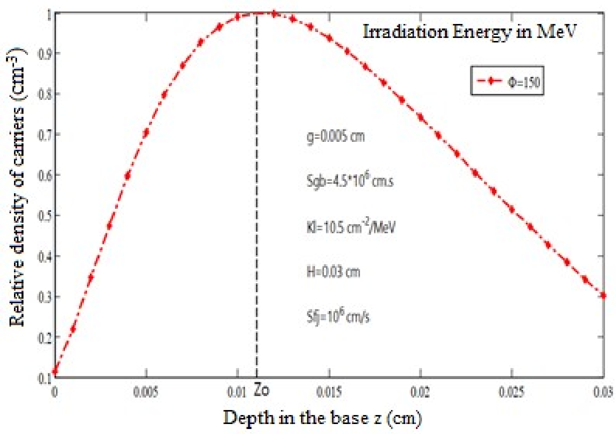

Figure.4: Relative density of carriers as a function of z-depth in the base.

If we consider a given operating point, the relative density of minority charge carriers shows positive, negative and zero gradients.
$Z_{0,av}$ characterizes the point of maximum minority charge carrier density and corresponds to the unit value of the relative density.
At $Z_{0,av}$ the gradient of the minority charge carrier density is zero. We are in open circuit and the space charge zone moves from $z = 0$ to $z = Z_{0,av}$.
The positive gradients of the density of minority charge carriers correspond to the zone from $z = 0$ to $z = Z_{0,av}$.
This zone is the site of an intense electric field that accelerates electric charges. No charge remains in this zone, which characterizes the extension of the space charge zone.
Negative gradients occur at $z \succ Z_{0,av}$, where carriers are blocked and recombine in volume.
The extension of the ZCE lies between $Z_{0,co}$ and $Z_{0,cc}$. $Z_{0,av}$ is determined by cancelling the derivative of the minority charge carrier density with respect to the variable z.

$$\left.\frac{\partial \delta(z, g, Sgb, Kl, \phi, Sb)}{\partial z}\right|_{Sf} = 0 \qquad \text{[Eq. 22]}$$

Since the junction is energized due to illuminance, we use the relationship (21) between voltage, charge and density to calculate the scattering capacity of the photocell in $Z_{0,av}$.

3.2. Effect of Grain Size g on the $Z_{0,av}$ Extension of the ZCE Space Load Area

Thus, we give in the following table (1) in which we present the different values of the scattering capacity of the photocell obtained for different values of the maximum of minority charge carriers when we assume that the recombination rate at the grain boundaries, the irradiation energy and the damage coefficient are constant.

Table 1: Some values of the capacity and extension of the space load zone $Z_{0,av}$ (cm) for six grain sizes and for illumination from the front side of the photocell

H=300µm; Sgb=4,5*10^6 cm.s^-1; Kl=10,5 cm^-2/MeV; Φ=150 MeV; Sf =10^6 cm/s.

$g(10\ \mu.m)$	2	18	20	23	25	30
$Z_{0,av}(10\mu.m)$	11	10	9	7	6	4.5
$V_{ph}(10^{-1}V)$	4.9	4.9	4.9	4.9	4.9	4.9
$E_{ZCE}(10^3 V.m^1)$	4.5	4.9	5.5	7.1	8.3	11
$C_{av}(10^5 nF.cm^{-2})$	1.4	1.9	2.2	2.7	3.2	3.5
$\delta(10^3.cm^{-3})$	2.43	3.36	4.17	4.76	5.16	5.42

In our analysis, we delve into the relationship between the capacity of solar cells and grain size, as illustrated in the accompanying table. By systematically varying the grain boundary recombination rate Sgb, irradiation energy, and damage coefficient, we can derive the corresponding scattering capacity of the photocell for specified grain sizes. This approach allows us to comprehensively understand how these parameters interact to influence the device's performance.
As we examine the data, it becomes evident that the capacity of the photocell exhibits distinct variations in response to changes in grain size. For each fixed value of the grain boundary recombination speed Sgb, along with constant irradiation energy and damage coefficient, we determine the resultant diffusion capacity of the photocell. Notably, for a grain size of $g = 20\,\mu m$, the diffusion capacitance remains high at $C_{av} = 1{,}38.10^5\,nF.cm^{-2}$ while the photovoltage stabilizes at_$V_{ph} = 4{,}99.10^{-1}V$, However, as_the grain size increases further, the photovoltage experiences a rapid increase, reaching a peak value of $C_{av} = 3{,}50.10^5\,nF.cm^{-2}$.

This behavior can be attributed to the interplay between grain size and charge carrier dynamics. Larger grain sizes tend to facilitate improved charge transport, reducing the likelihood of recombination at grain boundaries. Consequently, this leads to enhanced diffusion capacity and ultimately augments the photovoltage, which is critical for optimizing solar cell efficiency.
To visualize these relationships, we present fig.5, where we plot the inverse of the scattering capacity of the photocell as a function of the extension of the space charge zone $Z_{0,av}$.

This plot illustrates how the capacitive behavior of the photocell correlates with changes in the space charge

region, further emphasizing the significance of grain size and recombination dynamics in determining the overall performance of the solar cell.
In the current scientific landscape, understanding these relationships is crucial for advancing photovoltaic technology. Researchers are increasingly focused on optimizing grain structures to enhance charge carrier mobility and minimize losses due to recombination. As we move toward more efficient solar energy solutions, insights gleaned from such analyses will play a pivotal role in informing the design and fabrication of next-generation solar cells.

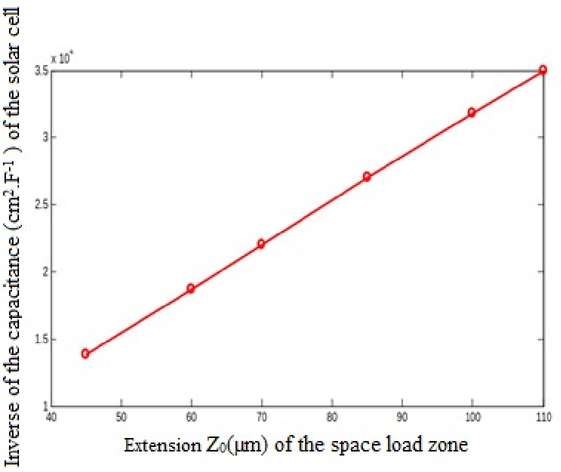

Figure.5: Inverse of the capacitance of the open-circuit solar cell as a function of the $Z_{0,av}$ (cm) extension $cm^2.F^{-1}$ of the space load area, when the grain size varies.
H=0,03 cm; Sgb=10^3 cm.s^{-1}; Kl=10,5 cm^{-2}/MeV; Φ=150 MeV; Sf=5.10^5 cm/s.

The inverse of the diffusion capacity is an affine function of the thickness of the space load area $Z_{0,av}$. It should be noted that the large values of the diffusion capacity correspond to the small values of the thickness of the space load zone. This curve shows that the junction of the photocell has the same properties of a capacitance.

3.3. Effect of Recombination Rate at Grain Boundaries Sgb on the $Z_{0,av}$ Extension of the ZCE Space Load Zone

The following table 2 shows the values of the scattering capacity of the photocell corresponding to the maximum point of the density of the minority charge carriers, the photovoltage and the accelerator electric field for different recombination rates at the grain boundaries

Table 2: Some values of the capacitance and extension of the load zone of space $Z_{0,av}$ (cm) for five recombination rates at the grain boundaries and for illumination from the front of the photocell,

H=300µm; g=0,003 cm; Kl=6 cm^{-2}/MeV; Φ=80 MeV; Sf =5.10^5 cm/s.					
$Sgb(10^2 cms^{-1})$	0.2	0.6	1.6	3.2	18
$Z_{0,av}(10\mu.m)$	3.8	5.2	7.2	8.7	9.9
$V_{ph}(10^{-1}V)$	4.9	4.9	4.9	4.9	4.9
$E_{ZCE}(10^3 V.m^1)$	13.1	9.6	6.9	5.7	5.1
$C_{av}(10^5 nF.cm^{-2})$	4.0	3.5	2.7	1.7	1.0
$\delta(10^3.cm^{-3})$	6.8	2.9	2.8	2.7	2.0

In this study, we investigate the effects of front-side illumination on bifacial solar cells with variable grain boundary recombination rates. Our findings reveal a direct correlation between increased recombination rates at grain boundaries and the extension of the space charge zone $Z_{0,av}$ Specifically, we observe that as recombination rates rise, there is a notable decrease in the density of minority charge carriers and a corresponding reduction in the diffusion capacity of the photocell.
When illumination is applied to the front face of the bifacial photocells, the variability in grain boundary recombination speeds plays a critical role in determining the electrical performance of the device. An increase in recombination rates not only extends the space charge zone $Z_{0,av}$ but also significantly diminishes the density of minority charge carriers, which are essential for maintaining efficient charge separation and collection within the solar cell.
For a specific grain boundary recombination rate $Sgb = 20 cm s^{-1}$, the diffusion capacity remains $C_{av} = 1{,}31.10^4 nF.cm^{-2}$ elevated initially but declines sharply as recombination rates continue to $C_{av} = 5{,}04.10^3 nF.cm^{-2}$ increase.
Moreover, we find that the photovoltage remains relatively constant across the extension of the space charge zone. However, with escalating recombination rates at the grain boundaries (denoted as Sgb, the overall performance of the photocell deteriorates.

- the increase in Sgb tends to push the solar cell toward a short-circuit operating condition,
- as the recombination processes at the junction-base interface create a significant void in minority charge carriers. In this scenario,
- the recombination effects dominate over the generation effects, compromising the cell's efficiency.

To further illustrate these findings, we present data in fig.6, where we plot the inverse of the capacitance as a function of $Z_{0,av}$. The curve's shape aligns with the characteristics of a plane capacitor, reinforcing our hypothesis regarding the capacitive behavior of the space charge zone under varying recombination conditions.
Overall, these results underscore the critical interplay between grain boundary dynamics and the electrical performance of bifacial solar cells, highlighting the importance of optimizing these parameters to enhance solar cell efficiency.

This curve in Figure6 of the diffusion capacity is a linear function of the extension of the space charge zone of the photocell, whose slope is strictly positive. This shows that the diffusion capacity increases with the extension of the space load zone.

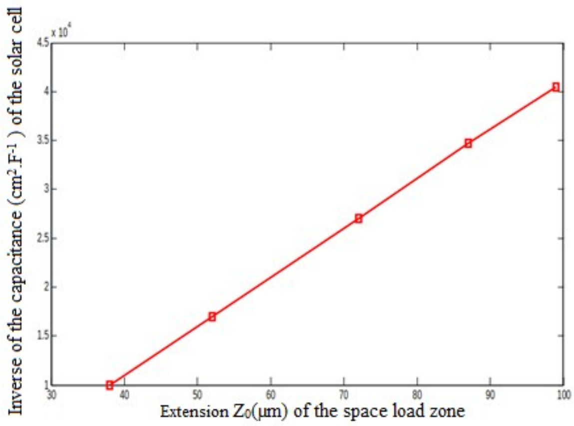

Figure.6: Inverse of the capacitance of the open-circuit solar cell as a function of the extension $Z_{0,av}$(cm) of the space load zone, when the recombination rate at the grain boundaries varies, H=0,03cm; g=0,003 cm; Kl=6 cm^{-2}/MeV; Φ=80 MeV.

4. Conclusion

In this study, we presented a robust technique for determining the extension $Z_{0,av}$ of the space charge zone within polycrystalline solar cells. Our findings demonstrate that elevated recombination rates at grain boundaries significantly reduce the diffusion capacity of the photocell. Conversely, an increase in grain size enhances this diffusion capacity, thereby improving the overall performance of the solar cell.

The investigation into the relative densities of minority charge carriers as a function of depth z within the base layer provides critical insights into the dynamics of the space charge zone. Specifically, the extension $Z_{0,av}$ serves as a pivotal parameter that characterizes both the open-circuit operating point of the solar cell and its overall quality.

Moreover, our analysis underscores the delicate balance between microstructural properties and electrical performance. By elucidating the relationships between grain size, recombination rates, and diffusion capacity, we contribute to the understanding of how these factors influence the efficiency of polycrystalline solar cells. A method for the determining the extension of the space charge zone has been presented. This method reveals that the increase in recombination rates at grain boundaries, from $Sgb = 20 cm s^{-1}$, leads to a decrease in the diffusion capacity, going from $C_{av} = 1,31.10^{4} nF.cm^{-2}$ to $C_{av} = 5042 nF.cm^{-2}$. On the other hand, the increase in the grain size from $g = 20\,\mu m$ to $g = 3,00\,10^{2}\,\mu m$ leads to an increase in this diffusion capacity up to . The analysis of the relative densities of the minority charge carriers as a function of the depth z in.

This work lays a foundation for future research aimed at optimizing solar cell designs, ultimately enhancing energy conversion efficiencies and advancing photovoltaic technology.

Overall, the methodology and results presented here not only deepen our understanding of space charge dynamics but also offer valuable guidance for improving the performance of next-generation solar cells.

REFERENCES

[1] M.L.Samb, S.Sarr, S. Mbodji, S. Gueye, M. Dieng and G. Sissoko, (2009), Etude en modélisation à 3-D d'une photopile au silicium en régime statique sous éclairement multispectrale : détermination des paramètres électriques. J. Sci; Vol. 9, N° 4, pp. 36 – 50; http ://www.cadjds.org

[2] S. Mbodji, A. S. maïga, M. Dieng, A. Wereme and G. sissoko, (2010), Renoval charge technic applied to a bifacial solar cell under constant magnetic field global Journal of pure and applied sciences Vol. 16, N°. 4: pp. 469-477. http://www.globaljournalseries.com

[3] S. Madougou, Nzonzolo, S. Mbodji, I.F. Barro and G. Sissoko, (2004), Bifacial silicon solar cell space charge region width determination by a study in modelling: effect of the magnetic field, J.Sci.Vol.4, N°3, pp. 116-123. http://www.cadjds.org

[4] F. I. Barro, S. Mbodji, M. Ndiaye, E. BA and G. Sissoko, (2008), Influence of grains size and grains boundaries recombination on the space-charge layer thickness z of emitter-base junction's n+-p-p+ solar cell Proceedings of the 23rd European Photovoltaic Solar Energy Conference, pp. 604-607. DOI:10.4229/23rdEUPVSEC-1CV.2.63 ; http://www.eupvsec-proceedings.com

[5] H. L. Diallo, A. S. Maïga, A. Wereme, G. Sissoko, (2008), New approach of both junction and back surface recombination velocity in a 3D modelling study of polycrystalline silicon solar cell. Eur. Phys. J. Appl. Phys. 42, pp. 203–211.

[6] A. Dieng, M.L. Sow, S. Mbodji, M.L. Samb, M. Ndiaye, M. Thiame, F.I. Barro and G. Sissoko, (2009), 3D Study of a Polycrystalline Silicon Solar Cell: Influence of Applied Magnetic Field on the Electrical Parameters. Proceedings of the 24th European Photovoltaic Solar Energy Conference, pp.473-476; DOI: 10.4229/24thEUPVSEC2009-1CV.4.16; http://www.eupvsec-proceedings.com

[7] B. Zouma, A. S. Maïga, M. Dieng, F. Zougmore, G. Sissoko,(2009), 3D Approach of spectral response for a bifacial silicon solar cell under a constant magnetic field Global Journal of Pure and Applied Sciences, Vol.15, N°1, pp.117-124; http://www.globaljournalseries.com

[8] S. Mbodji, M. Dieng, B. Mbow, F. I.Barro and G. Sissoko, (2010), Three dimensional simulated modelling of diffusion capacitance of polycrystalline bifacial silicon solar cell. Journal of Applied Sciences and Technology (JAST) Vol. 15, Nos.1&2, pp. 109 - 114; http://www.inasp.info/ajol

[9]. J. Oualid and C. M. Singal; (1984), Influence of illumination on the grain boundarie recombination velocity in silicon. J. Appl. Phys. 55(4), pp. 1195-1205.

[10] S. Mbodji, M. Dieng, B. Mbow, F. I.Barro and G. Sissoko, (2010), Three dimensional simulated modelling of diffusion capacitance of polycrystalline bifacial silicon solar cell. Journal of Applied Sciences and Technology (JAST) Vol. 15, Nos.1&2, pp. 109 - 114; http://www.inasp.info/ajol

[11] Mayoro Dieye, Nacire Mbengue and Awa Dieye, 3-D modeling of the influence of irradiation on the electrical power of a single-sided polycrystalline silicon photocell subjected to multi-spectral illumination, European Journal of Advances in Engineering and Technology (EJAET); 2022, 9(9): 16 - 21;
[12] Mayoro Dieye, Awa Dieye and Nacire Mbengue, Three-Dimensional Modeling Study of the Effect of Irradiation on the Density of Minority Carriers for a Single-Face Polycrystalline Silicon Photocell under Multispectral Illu,ination, Journal of Scientific and Engineering Research (JSER); 2022, 9(10): 21 - 27;
[13] Mayoro Dieye, Senghane Mbodji, Martial Zoungrana, Issa Zerbo, Biram Dieng and Grégoire Sissoko, A 3D Modeling of Solar Cell's Electric Power under Real Operating Point,, World Journal of Condensed Matter Physics, 2015, 5, 275-283.
http://www.scrip.org/journal/wicmp
[14] R. J. Walters and G. P. Summers; (2002), Space Radiation Effects in Advanced Solar Cell Materials and Devices Mat. Res. Soc. Symp. Proc. Vol. 692, pp. 569-580.
[15] R. K. Ahrenkiel, D. J. Dunlavy, H. C. Hamaker, R. T. Green, C. R. Lewis, R. E. Hayes, H. Fardi; (1986), Time-of-flight studies of minority-carrier diffusion in AlxGa-xAs homojunctions. J. Appl. Phys. 49(12).
[16] Mbodji, S., Ly, I., Diallo, H.L., Dione, M.M., Diasse, O. and Sissoko, G. (2012) Modeling Study of N+/P Solar Cell Resistances from Single I-V Characteristic Curve Considering the Junction Recombination Velocity (Sf). Research Journal of Applied Sciences, Engineering and Technology, 4, 1-7.
[17] M.A. Ould El Moujtaba, M. Ndiaye, A. Diao, M. Thiame, I.F. Barro and G. Sissoko. (2011), Theoretical Study of the Influence of Irradiation on a Silicon Solar Cell under Multispectral Illumination. Research Journal of Applied Sciences, Engineering and Technology, 4(23): pp. 5068-5073.
[18] Mayoro Dieye, Awa Dieye and Nacire Mbengue, Influence of illumination grain size and grain boundary recombination velocity on the facial solar cell diffusion capacitance, European Journal of Advances in Engineering and Technology, 2022, 9(9):22-27
Available online www.ejaet.com
[19] Y. L. B. Bocande, A. Correa, I. Gaye, M. L. Sow and G. Sissoko, (1994), Bulk and surfaces parameters determination in high efficiency Si solar cells. Renewable Energy, Vol 5, part III, pp. 1698-1700, (1994)- Pergamon, 0960-1481.
[20] M .C Halder and T.R. Williams, (1983), Grain boundary effects in polycrystalline Silicon SolarCells I. Solution of the three- Dimensional diffusion equation by the Green's function method, Solar Cells, Vol. 8, No 3, pp. 201- 223.
[22] M. M. Deme, S. Mbodji, S. Ndoye, A. Thiam, A. Dieng and G. Sissoko, (2010), Influenceof illumination incidence angle, grain size and grain boundary recombination velocity on the facial solar cell diffusion capacitance; Revue des Energies Renouvelables Vol. 13 N°1 (2010), pp. 109-121
[23] G. Sissoko, E. Nanéma, A. Corréa, P. M. Biteye, M. Adj, A. L. Ndiaye, (1998), Silicon Solar cell recombination parameters determination using the characteristic. Renewable Energy, Vol-3, pp.1848-1851 Elsevier Science Ltd, 0960-1481/98/#.
[24] G. Sissoko, C. Museruka, A. Correa, I. Gaye, A. L. Ndiaye, (1996), Light spectral effect on recombination parameters of silicon solar cell. In Proceedings of the World Renewable Energy Congress, pp. 1487-1490.
[25]Barro, F.I., S. Mbodji, A.L. Ndiaye, I. Zerbo, S. Madougou, F. Zougmore and G. Sissoko, (2004), Bulk and Surface Parameters Determination by a Transient Study Bifacial Silicon Solar Cell under constant White Bias Light. Proc. of 19th European photovoltaic Conference and Exhibition June, Paris, France, pp: 447- 450.
[26] Mayoro Dieye, Nacire Mbengue and Awa Dieye, 3-D modeling of the influence of irradiation on the electrical power of a single-sided polycrystalline silicon photocell subjected to multispectral illumination, European Journal of Advances in Engineering and Technology, 2022, 9(9):16-21
Available online www.ejaet.com
[27] Dhariwal SR, Mehrotra DR. Photocurrent and photovoltage from polycrystalline p-n junction Solar Cells. Solar Cells. 1988;25(3):223-33.
DOI: 10.1016/0379-6787(88)90062-2
[28] El Ghitani H, Martinuzzi S. Influence of dislocations on electrical properties of large grained polycrystalline silicon cells. I. Model. J Appl Phys. 1989;66(4):1717-22. DOI: 10.1063/1.344392